JOURNAL OF GEOPHYSICAL RESEARCH, VOL. 113, C06014, doi:10.1029/2007JC004383, 2008

Click Here for Full Article

Revisiting heat and salt exchange at the ice-ocean interface: Ocean flux and modeling considerations

M. G. McPhee,[1] J. H. Morison,[2] and F. Nilsen[3]

Received 12 June 2007; revised 28 February 2008; accepted 17 March 2008; published 14 June 2008.

[1] Properly describing heat and salt flux at the ice/ocean interface is essential for understanding and modeling the energy and mass balance of drifting sea ice. Basal growth or ablation depends on the ratio, R, of the interface heat exchange coefficient to that of salt, such that as R increases so does the rate-limiting impact of salt diffusion. Observations of relatively slow melt rates in above freezing seawater (plus migration of summer "false bottoms") suggest by analogy with laboratory studies that double diffusion of heat and salt from the ocean is important during the melting process, with numeric values for R estimated to range from 35 to 70. If the same double-diffusive principles apply for ice growth as for melting (i.e., if the process is symmetric), supercooling (possibly relieved by frazil crystal production) would occur under rapidly growing ice, yet neither extensive supercooling nor frazil accumulation is found in Arctic pack ice with limited atmospheric contact. Physical properties and turbulent fluxes of heat and salt were measured in the relatively controlled setting of a tidally driven Svalbard fjord, under growing fast ice in late winter. The data failed to show supercooling, frazil production, or enhanced heat flux, suggesting that the double diffusive process is asymmetric. Modeling results compared with measured turbulent fluxes imply that $R = 1$ when ice freezes; i.e., that double-diffusive tendencies are relieved at or above the immediate interface. An algorithm for calculating ice/ocean heat and salt flux accommodating the different processes is presented, along with recommended ranges for the interface exchange coefficients.

Citation: McPhee, M. G., J. H. Morison, and F. Nilsen (2008), Revisiting heat and salt exchange at the ice-ocean interface: Ocean flux and modeling considerations, *J. Geophys. Res.*, *113*, C06014, doi:10.1029/2007JC004383.

1. Introduction

[2] At high latitudes, sea ice often controls the thermodynamics of the ocean surface by providing an effective insulating cover during winter and by greatly reducing absorption of incoming short-wave radiation in summer. In recent years, significant decreases in the observed extent and thickness of Arctic sea ice have focused attention on the possibly precarious state of the perennial ice pack [*Rothrock et al.*, 1999; *McPhee et al.*, 1998; *Holland et al.*, 2006] and on identifying the important factors for maintaining a sea-ice cover. Data from the yearlong (1997–1998) Surface Heat Budget of the Arctic (SHEBA) project in the western Arctic demonstrated that ice/ocean heat and salt exchange are an important component of the mass balance of sea ice. Application of a model [*McPhee*, 2008] developed to estimate regional ice/ocean exchange in the western Weddell Sea to the SHEBA upper ocean data implied an average basal heat flux of about 7 W m^{-2} during the SHEBA year, close to the estimate of *Perovich and Elder* [2002] based on mass balance measurements in undeformed, multiyear ice. Thus the annual heat loss from the ocean was roughly 220 MJ m^{-2}, which in the absence of other factors, is enough energy to melt up to 0.9 m of sea ice.

[3] Growing ice rejects as much as 80% of the salt in the water from which it forms, and after surviving a summer, sea ice will often exhibit salinities as low as 1–2 units on the practical salinity scale (hereafter abbreviated "psu"). When ice is present, near-surface water temperature rarely reaches the freezing temperature of brackish water with observed ice salinities, so it is clear that salt diffusion must play an important role in the heat and mass balance at the interface. Familiar examples occur when salt is used to clear snow from a roadway or to harden ice cream. For cold seawater, molecular thermal diffusivity exceeds haline diffusivity by a factor of about 200; hence it is reasonable to suspect that heat and mass exchange at the ice/water interface are subject to "double diffusion," i.e., unequal transfer rates for heat and salt.

[4] The first direct measurements of turbulent heat flux in the ocean boundary layer under drifting pack ice during the Marginal Ice Zone Experiment (MIZEX) in 1984 [*McPhee et al.*, 1987], indicated that in contrast to momentum flux, heat exchange under hydraulically rough sea ice was governed by thin sublayers near the interface where

[1] McPhee Research Company, Naches, Washington, USA.
[2] Polar Science Center, University of Washington, Seattle, Washington, USA.
[3] University Centre in Svalbard, Longyearbyen, Norway.

Copyright 2008 by the American Geophysical Union.
0148-0227/08/2007JC004383$09.00

molecular exchange was important, i.e., that the thermal and haline molecular diffusivities played a significant role. This view was bolstered by observations from the yearlong Arctic Ice Dynamics Joint Experiment (AIDJEX) ice camps [*Maykut and McPhee*, 1995] and more recently the Surface Heat Budget of the Arctic (SHEBA) and shorter summer projects [*McPhee et al.*, 2003] indicating that temperature of the Arctic mixed layer was often considerably above freezing for extended periods during the summer months, even when ice covered most of the surface. In the absence of the transition sublayers, heat exchange would be so rapid that solar energy entering the mixed layer during summer would be transferred to the ice in a matter of hours rather than days, with little sensible heat storage in the well mixed layer [*McPhee et al.*, 1987].

[5] Less direct (but no less convincing) evidence for the importance of double diffusion during melting comes from observations of the vertical migration of ''false bottoms.'' These form under pack ice during summer when fresh meltwater becomes trapped in concavities at the ice underside and are observed regularly. *Notz et al.* [2003] successfully modeled observations of false-bottom persistence and migration, when their model accounted for relatively strong double diffusive effects as described below. Without double diffusion at the interface, their model results suggested that false bottoms would be so ephemeral as to be rarely observed.

[6] As pointed out by *Mellor et al.* [1986] and in more detail by *Steele et al.* [1989], if double diffusive effects are as strong during freezing as they apparently are during melting, then unequal heat and salt transfer could lead to substantial supercooling (i.e., cooling water to temperatures below the in situ freezing point). Consider ice formation over a well-mixed water layer initially at its freezing temperature. As water salinity increases due to salt rejected from the ice, the freezing temperature lowers; thus to maintain the water layer at freezing in the face of downward salt flux requires a small upward heat flux in the ocean, with a small reduction in ice growth. We show in section 2.1 that such a balance occurs when the ratio of heat and salt exchange coefficients across the transition sublayers is one. During melt, this ratio is apparently much greater than unity, so if the process is symmetric for freezing in the sense that the exchange coefficients for heat and salt remain the same, then in the example the transfer of salt away from the interface would be inhibited relative to heat transfer, increasing the temperature contrast between the interface and far field and consequently the upward ocean heat flux. The result is to extract more heat from the water column, which provides a larger proportion of the heat needed to balance upward conduction in the ice. If the water column is already at freezing, it will supercool. Since less latent heat release is required to balance upward conduction, ice growth is slowed. If sufficient nucleation sites existed in the water, frazil crystals would form, and in a turbulent environment would be dispersed in some manner through the ice-ocean boundary layer.

[7] Using an ice-ocean model in which the double-diffusive tendency was as great during freezing as melting, *Steele et al.* [1989] inferred that a sizable fraction of the ice accretion would come from frazil ice. In a combined sea ice/ocean modeling study with multiple ice thickness categories, *Holland et al.* [1997] demonstrated that this effect could significantly increase the equilibrium thickness of the modeled ice pack. In their model, supercooled water was converted to frazil immediately and distributed through the boundary layer so that all thickness categories received frazil accretion equally. Compared with straight congelation growth in each thickness category, this resulted in less rapid accretion under thin ice, hence steeper temperature gradients and overall more upward heat transfer.

[8] The upshot of these studies was that if the double-diffusive tendency was symmetrical for melting and freezing, then there ought to be ample evidence of significant supercooling during rapid ice growth and/or frazil structure in the fabric of multiyear ice cores. It turns out that neither is very prevalent in observations from Arctic pack ice. Supercooling of approximately 4 mK (i.e., observation of water temperature 0.004 kelvins below its freezing temperature, which depends on salinity and pressure) was reported near ice island ARLIS 2 by *Untersteiner and Sommerfeld* [1964], using a novel measurement technique that did not require accurate salinity determination. Because of the dependence of freezing temperature on pressure, it is not uncommon to encounter water that is supercooled near the surface if it has been in contact with ice at depth, e.g., in the vicinity of ice shelves or thick icebergs (such as ARLIS 2). *Lewis and Perkin* [1983] reported supercooling of as much as 8 mK based on temperature and salinity measurements made with modern instrumentation north of Svalbard, in a region with large horizontal gradients in temperature and salinity. Most earlier reports of significant supercooling in the Arctic [e.g., *Coachman*, 1966] have been questioned regarding the methods of determining salinity if ice crystals were present [*Lewis and Lake*, 1971]. Model results described above predict either much stronger supercooling than has been observed, or production of significant frazil ice, up to 30% of the total ice production [*Steele et al.*, 1989]. By examining the fabric in thin sections of sea ice, it is relatively straightforward to distinguish between columnar ice accreted by congelation growth (with horizontal crystal c-axis orientation) versus that from frazil. In Arctic sea ice and fast sea ice in both hemispheres, frazil is thought to account for only about 5% of total ice volume, found mainly near the surface produced during initial ice formation [*Weeks and Ackley*, 1986].

[9] The discrepancy between models that emphasized the potential impact of double diffusion during freezing, and the lack of much evidence for supercooling or frazil production when the interface was not in direct contact with the atmosphere, provided the rationale for an experiment designed to investigate details of freezing and its impact on the upper water column in the relatively controlled environment of tidally driven flow under fast ice in a Svalbard fjord. The present work has two objectives. First, we seek to determine whether double diffusive effects are apparent in oceanographic measurements made under growing ice in VanMijenfjorden, Svalbard, in late winter, 2001. Second, we incorporate our results from that study along with other recent data to recommend a parameterization of heat and salt exchange at the ice/ocean interface for use in ice/ocean models. Section 2 reviews a theoretical approach to the problem, including derivation of the ''three-equation model'' and its implications for rapid melting. Section 3

describes turbulence and mean quantity measurements made when ice was freezing, during a field program including University Centre in Svalbard (UNIS) student participation. Section 4 presents results from a simple numerical modeling simulation that compared with measurements of section 3, strongly suggests asymmetry in the double-diffusive character of the ice/ocean interface. Finally, in section 5 we recommend an algorithm for parameterizing the process in model studies.

2. Background

2.1. Heat and Mass Transfer Across Hydraulically Rough Surfaces

[10] The MIZEX heat flux measurements in 1984 indicated unexpectedly low values for ocean heat flux and basal melting, given the observed elevation of mixed layer temperature and turbulent stress. Following consultation with G. Mellor and L. Kantha (personal communication, 1985), we adapted results from laboratory studies of fluid heat and mass exchange across hydraulically rough surfaces [*Yaglom and Kader*, 1974, hereinafter referred to as YK; *Owen and Thomson*, 1963, hereinafter referred to as OT; *Incropera and DeWitt*, 1985] to the ice/ocean interface [*McPhee et al.*, 1987]. This approach suggested that the nondimensional temperature change (an inverse Stanton number) across a transition sublayer where molecular effects governed should vary as follows:

$$\Phi_T = \frac{(T_{ts} - T_0)u_{*0}}{\langle w'T' \rangle_0} \propto Re^{1/2} Pr^n \tag{1}$$

where $T_{ts} - T_0$ is is the change in temperature across the transition sublayer (subscript 0 refers to interface values), u_{*0} is the interfacial friction velocity; $\langle w'T' \rangle_0$ is the kinematic turbulent heat flux (i.e., heat flux divided by the product of density and specific heat); *Re* is the Reynolds number of the flow; and *Pr* is the Prandtl number (ν/ν_T, where ν is molecular viscosity and ν_T is molecular thermal diffusivity). A similar relation holds for the nondimensional change in salinity across the transition sublayer, where the Prandtl number is replaced by the Schmidt number (ν/ν_S, where ν_S is molecular salt diffusivity).

[11] According to (1), Φ_T should vary as the square root of the Reynolds number. YK defined the Reynolds number as $Re_* = 30 z_0 u_{*0}/\nu$, where the length scale for the transitional sublayer was taken to be the scale of the roughness elements, approximately 30 times the hydraulic roughness, z_0. However, data from several projects with underice roughnesses ranging from hydraulically smooth to several centimeters have shown no discernible dependence on Re_* [e.g., *McPhee et al.*, 1999]; hence for sea ice, (1) is more appropriately expressed as

$$\Phi_{T(S)} \propto \left(\nu/\nu_{T(S)}\right)^n \tag{2}$$

YK suggested that the exponent *n* in (2) is 2/3 (the same as obtained from the analytic Blasius solution for purely laminar flow); whereas OT found it to be about 0.8. Its value is critical for estimating double diffusive impact as discussed below.

2.2. Ice-Ocean Interface

[12] The unique double-diffusive character of thin fluid layers near the melting ice/seawater interface is illustrated as follows [e.g., *Mellor et al.*, 1986; *McPhee*, 1992; *Morison and McPhee*, 2001; *Notz et al.*, 2003]. From conservation of enthalpy in a thin volume enclosing the interface, kinematic turbulent heat flux from the ocean is approximately

$$\langle w'T' \rangle_0 = w_0 Q_L + \dot{q} \tag{3}$$

where $w_0 = -(\rho_{\mathrm{ice}}/\rho)\,\dot{h}$ is the isostatically balanced ice melt rate ($\dot{h}$ is ice growth rate, ρ_{ice} and ρ are ice and water density, respectively), Q_L is latent heat of fusion (i.e., latent heat, a function of brine volume, hence salinity) divided by the specific heat of seawater, c_p, and $\dot{q}$ is heat conduction near the base of the ice column divided by the product ρc_p. Similarly, salt conservation is given by the advective balance

$$\langle w'S' \rangle_0 = w_0 (S_0 - S_{ice}) \tag{4}$$

where S_0 is salinity at the interface, and S_{ice} is ice salinity. By dimensional analysis, the turbulent heat and salt flux may be parameterized in terms of interface exchange coefficients α_h and α_S:

$$\begin{aligned} \langle w'T' \rangle_0 &= \alpha_h u_{*0} \delta T \\ \langle w'S' \rangle_0 &= \alpha_S u_{*0} \delta S \end{aligned} \tag{5}$$

where $\delta t = T_w - T_0$ and $\delta S = S_w - S_0$ are differences between the far-field and interface temperature and salinity.

[13] If $\dot{q}$, S_{ice}, u_{*0}, and far-field T_w and S_w are specified, (2)–(5) may be combined with the freezing line approximation $T_0 = -mS_0$ to provide a system of three equations, reducing, e.g., to a quadratic equation for interface salinity:

$$mS_0^2 + \left(T_w - \frac{\dot{q}}{\alpha_h u_{*0}} + \frac{\alpha_S Q_L}{\alpha_h} - mS_{ice}\right) S_0 - S_{ice}\left(T_w - \frac{\dot{q}}{\alpha_h u_{*0}}\right) - S_w Q_L \frac{\alpha_S}{\alpha_h} = 0 \tag{6}$$

from which the interface fluxes follow via (3) and (4). It is clear from (6) that flux magnitudes depend on the ratio of the exchange coefficients, α_h/α_S. If the far-field temperature is nearly the same as the temperature at the far extent of the transition sublayer, then from (2) $\alpha_{h(s)} \propto (\nu/\nu_{T(S)})^{-n}$, implying that the exchange coefficient ratio goes as $R = \alpha_h/\alpha_S \approx (\nu_T/\nu_S)^n$. *R* may be considered a measure of the strength of double diffusion, i.e., as *R* increases heat transfer increases relative to salt transfer, and the rate-limiting impact of salt diffusion becomes stronger. For $R = 1$, there is no double-diffusive tendency. As summarized by *Notz et al.* [2003], combining results from laboratory studies, from rapid melting in the marginal ice zone, and from consideration of "false bottoms" under summer pack ice, suggests that $35 \leq R \leq 70$, when the energy balance at the interface dictates melting.

[14] In principle, measurements during rapid melting of turbulent fluxes of momentum, heat, and salt near the interface, along with far-field temperature and salinity,

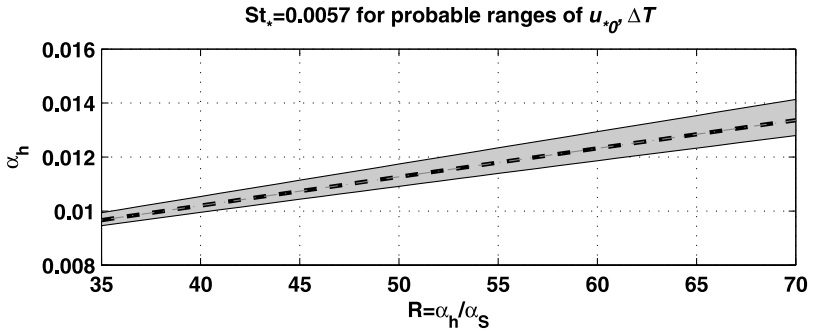

Figure 1. Envelope of possible values for α_h as a function of double-diffusive strength for a plausible range of u_{*0} and ΔT, providing the same kinematic heat flux as the bulk formula (7). The heavy solid curve is the locus of α_h values for $u_{*0} = 0.01$ m s^{-1} and $\Delta T = 0.3$ K, typical of Arctic pack ice in summer.

would suffice to determine R provided the interface is at the liquidus. It is difficult in practice to achieve unequivocal values because (1) precise measurement of salinity flux is difficult and (2) rapid melting of sea ice, particularly pack ice in the marginal ice zone, often occurs in markedly heterogeneous environments with rapid temporal variation and large horizontal gradients.

[15] In contrast, there is a considerable database from which to assess a bulk exchange coefficient (often referred to as a Stanton number) relating heat flux measured near the surface to the product of far-field (mixed-layer) temperature and salinity, along with u_{*0}, namely,

$$St_* = \frac{\langle w'T' \rangle_0}{u_{*0}\Delta T} \tag{7}$$

where $\Delta T = T_{ml} - T_f(S_{ml})$ is the elevation of mixed-layer temperature above freezing. (In all but the most extreme conditions, the difference between T_{ml} and T_w is dwarfed by the temperature change across the transition sublayer.) Measurements in the ice/ocean boundary layer, encompassing a relatively wide range of undersurface stress, heat flux, and roughness conditions, have documented a surprisingly uniform value for St_*, typically ranging between 0.005 and 0.006 [*McPhee et al.*, 1987; *McPhee*, 1992; *McPhee et al.*, 1999]. The estimated value from the yearlong SHEBA project in the western Arctic was 0.0057 ± 0.0004 [*McPhee et al.*, 2003].

[16] For R in the range suggested by *Notz et al.* [2003], it is important to note the distinction between α_h and St_*. The interplay between stress and thermal driving precludes a one-to-one relation between α_h and St_* for all conditions; however, for a plausible range of forcing values ($5 \leq u_{*0} \leq 15$ mm s^{-1}; $0.05 \leq \Delta T \leq 0.5$ K), the interface equations may be solved iteratively for an envelope of values for α_h that produce the same heat flux as (5) for $St_* = 0.0057$ (Figure 1). Note that over most of the range of R, α_h is more than twice as large as St_*. The reason for this is straightforward: if ice is melting, then interface salinity S_0 will be less than S_{ml}, with the difference increasing with the strength of double diffusion, i.e., increasing R. Consequently, $\delta T < \Delta T$ (since $T_0 > T_f(S_{ml})$); and from (5) and (7), $\Delta T/\delta T = \alpha_h/St_*$.

[17] As described in section 1, when ice is freezing instead of melting, an actively double-diffusive interface would extract heat from the upper ocean faster than adding salt, with the possibility of substantial supercooling and possible frazil ice formation. Yet there is scant evidence from previous pack ice studies, including the yearlong SHEBA project in 1997–1998 when the upper ocean was often very close to its freezing temperature, that either extensive supercooling or frazil production occurs under freezing conditions, as long as a thin ice cover prevents direct contact between the atmosphere and liquid ocean.

3. Turbulence Measurements During the 2001 VanMijenfjorden Exercises

[18] On the basis of previous experience from University Centre in Svalbard (UNIS) student field exercises on Svalbard fjords, we reasoned that tidal flow under relatively thin and horizontally uniform fast ice in late winter would provide a good laboratory for studying exchanges at the ice/ocean interface during freezing conditions. In March 2001, we encountered conditions in VanMijenfjorden (VMF), Svalbard, with seawater close to freezing, and ice growth at a surface in contact with a turbulent boundary layer forced by gentle tidal flow. Our station was established at location 77°48.80′N, 15°54.25′E, in about 50 m of water offshore from the navigation marker designated Dom Miguel (DM). The experiment included a "turbulence instrument cluster" (TIC) comprising Sea-Bird Electronics temperature, conductivity and microstructure conductivity sensors, plus a Sontek acoustic-backscatter three-dimensional current meter (ADVOcean), mounted 1 m below the ice/ocean interface. The TIC was deployed during the primary measurement program from about midday on 7 March to midday on 10 March 2001 (year days 66.5 to 69.5).

[19] The primary goal of the turbulence project was to assess R (the double-diffusive strength) during a time when the heat balance at the interface dictated reasonably rapid ice growth, by measuring fluxes of momentum, heat, and salt near the interface, as described above. The turbulence data were processed in 15-min "realizations" following procedure described previously [e.g., *McPhee*, 2002; *McPhee*, 2008]. Measured tidal velocities at DM ranged up to about 0.08 m s^{-1}. To gauge the dependence of turbulence properties on mean current, the flux measurements (Figure 2) were classified according to mean current speed in 0.01 m s^{-1} bins from 0.025 to 0.085 m s^{-1}. The

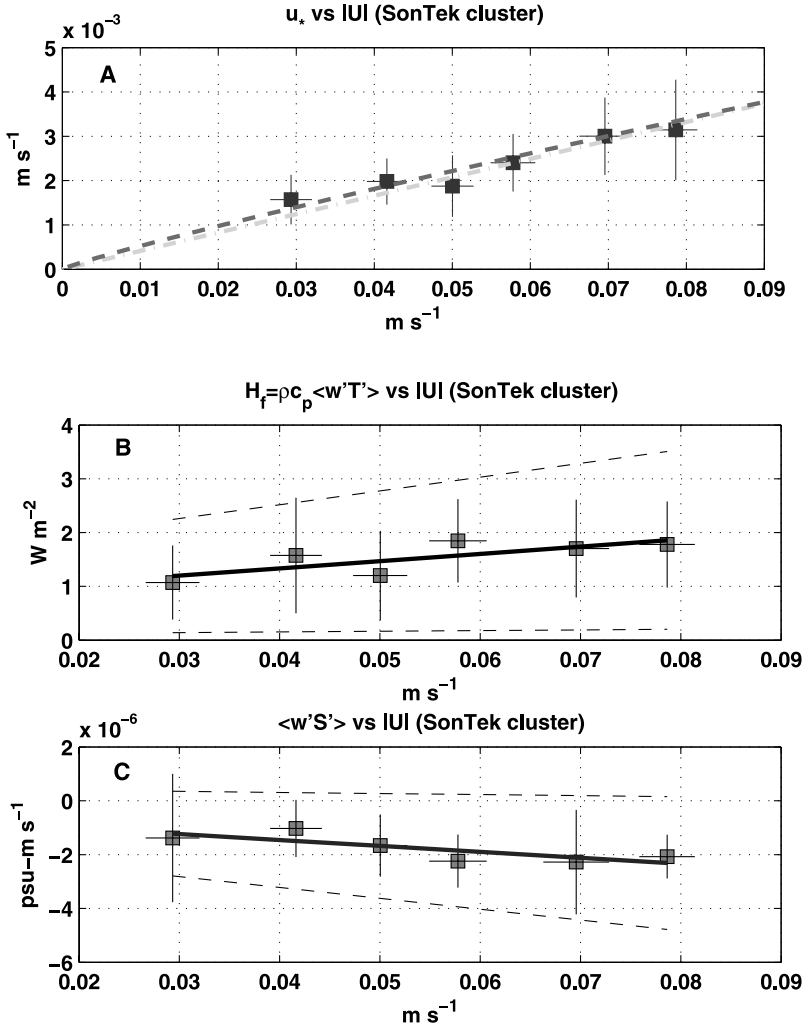

Figure 2. (a) Friction velocity versus current speed 1 m below ice (square symbols, error bars represent ±1 standard deviation of the 15-min realizations in each bin). The dot-dashed line is a linear fit through the origin, while the dashed curve is u_{*0} for a hydraulically smooth ice undersurface [*Hinze*, 1975]. (b) Turbulent heat flux as a function of current speed. Error bars as above. The solid line is a regression line with 90% confidence intervals indicated by dashed lines. (c) Same as Figure 2b except turbulent salinity flux $\langle w'S' \rangle$.

red curve in Figure 2a is from the "law-of-the-wall" for a hydraulically smooth surface:

$$\frac{U_{1m}}{u_{*0}} = \frac{1}{\kappa} \log \frac{u_{*0}}{\nu} + 4.9 \qquad (8)$$

where κ is von Kàrmàn's constant [*Hinze*, 1975], indicating that the undersurface was indeed very smooth. The regression lines for heat and salinity flux in Figures 2b and 2c show a slight increase in flux magnitude with current speed but are barely distinguishable from zero at the 90% confidence level, which seems at first surprising in light of the obvious dependence of u_* on U. However, as discussed below in the context of modeling, this probably means that the turbulence scales in the ocean boundary layer were responding more to convection associated with salt rejection than from boundary layer shear in the gentle tidal currents.

[20] A small underwater remotely operated vehicle (ROV) equipped with a specially designed Sea-Bird Electronics conductivity-temperature-depth (CTD) system made frequent, highly detailed profiles through variable depths up to 14 m, providing accurate mixed layer properties, supplemented by TIC measurements of temperature and salinity 1 m below the ice.

[21] The site occupied during the main field program was revisited about 10 days later (16–19 March) during a UNIS student exercise with turbulence measurements and CTD profiling. An additional follow-up CTD study was performed at the end of March. Details are presented in the UNIS AGF-211 student report "Measurements in Van Mijenfjorden, March–April 2001" (unpublished manuscript, University Center in Svalbard, Longyearbyen, Norway, 2001, hereinafter referred to as "AGF student report"). Included are data from an RCM9 current meter deployed at 10 m depth, operating for the entire period (Mattsson and Slubowska, AGF student report, 2001). The students also measured ice temperature profiles from cores at DM on 18–

21 March and again on 31 March (Halkola and Puhakka, AGF student report, 2001).

4. Numerical Ice/Ocean Model Analysis

[22] In order to illustrate the strength of double-diffusive effects when ice is freezing (as opposed to melting), we carried out an idealized modeling study of ice/ocean interaction during the entire spring 2001 VMF campaign, including the student exercises.

[23] The ocean model utilizes "local turbulence closure" [*McPhee*, 1999, 2002]. Beginning from specified initial temperature and salinity profiles, the one-spatial-dimensional model steps forward in time via a leapfrog algorithm [*Mellor et al.*, 1986], forced by specified friction velocity (u_{*0}) and by buoyancy flux calculated with an interface submodel for each time step using a solution of the quadratic formula (6), from a combination of u_{*0}, temperature and salinity at the uppermost grid point in the model, and specified heat conduction in the ice lower column, assuming water at the immediate interface is at its freezing point. As described above, this algorithm depends on R, so that as the ratio increases, so does the double-diffusive tendency, i.e., heat is extracted from the water column faster than salt is added, with potential for supercooling and/or frazil production.

[24] Three model runs were performed with identical initial conditions and temporal forcing, but with different double-diffusion strengths used in the interface submodel: $R = 1$, no double diffusion; $R = 5$, with slight double-diffusive tendency; and $R = 35$ with relatively strong double diffusion strength (but near the low end of the range suggested by *Notz et al.* [2003] for melting ice). The model runs are referred to below as R_1, R_5, R_{35}, respectively.

4.1. Model Initialization and Forcing

[25] Setting the initial temperature and salinity values was somewhat problematic because equipment problems with the UNIS CTD during the 6–10 March exercise prevented sampling the entire water column. Profiles measured on March 17 and 18 as part of the student exercise (Takayama et al., AGF student report, 2001) showed a relatively well-mixed layer to about 40 m, with a slight gradient in salinity below to around 34.42 psu near the bottom, and temperature nearly isothermal with bottom value about −1.88°C. By then the mixed layer was significantly more saline than during the earlier (7–10 March) period. After estimating the amount of deepening in 10 days using the model as described below, we specified initial *T/S* profiles with a mixed layer 33 m thick and mean values as measured on 7 March ($T_{ml} = -1.874$°C, $S_{ml} = 34.365$ psu) with linear gradients to the bottom, assuming that bottom characteristics changed little over the 10 intervening days.

[26] Measured values of u_{*0} under the fast ice were small (mean value, 1.9 mm s^{-1}, corresponding to an interface stress of about 4 mPa), responding to a relatively weak tidal flow at the DM site. Stress measured during the student campaign was slightly smaller. Our onsite instruments provided a relatively short record of near surface velocity, which combined with measured stress, indicated that the ice undersurface was hydraulically smooth (Figure 2). We then used a digitized version of a continuous RCM9 current record to construct a time series of u_{*0} from the hydraulically smooth stress condition, based on the measured current speed, assuming mean shear between 1 and 10 m to be small. For a day and a half before the RCM record started, the tidal velocity was extended backward in time, based on TIC and acoustic Doppler profiler measurements.

[27] Ice temperature measurements in early March indicated a relatively strong thermal gradient in the upper ice column, but the profiles appeared to taper toward the bottom to a somewhat lesser value, equivalent to conduction near the base of the ice of roughly 20 W m^{-2} upward. Presumably, the steeper gradient observed higher in the ice column indicates continued cooling of the ice mass, consistent with relatively cold air temperatures in March. Student temperature gradient measurements at DM on 18–21 March and again on 31 March showed a fairly consistent thermal gradient of about −10 K m^{-1} near the bottom of the cores; we therefore specified $\dot{q} = 5 \times 10^{-6}$ K m s^{-1}, equivalent to a conductive heat flux of about 21 W m^{-2}, held constant throughout the simulation.

4.2. Model Results

[28] The model was run over a domain 50 m deep with 200 equally spaced vertical grid points using a 7.5-min time step over a 24-day period from 7 to 31 March (days 66–90). Fluxes at the bottom of the domain were set to zero. For $R = 1$ ($n = 0$), there is no double diffusive tendency, and in an idealized scenario with water column temperature initially at the liquidus, the basal heat flux would just be that needed to maintain the mixed layer at freezing as its salinity increased. In fact, the initial water column based on the 7 March measurements, was about 12 mK above its surface freezing temperature; thus there was a small reservoir of oceanic heat available at the outset.

[29] Modeled friction velocity a meter below the ice, compared with periods when stress measurements were made (Figure 3), indicates that estimating surface stress by assuming a hydraulically smooth undersurface was not unreasonable. Only results for R_1 are shown: the others were essentially similar. At these low levels, the impact of u_{*0} is relatively minor in the model compared with w_*, the convective velocity associated mainly with destabilizing surface buoyancy flux. A separate model run, holding u_{*0} constant at its average value (1.9 mm s^{-1}) measured 1 m below the ice during the primary March exercise produced only minor variation in the model results.

[30] The model was initialized with ice thickness equal to 0.7 m, based on measurements during the initial deployment. Over the 24-day run with constant 21 W m^{-2} upward conductive heat flux near the ice undersurface, modeled ice growth ranged from 158 mm for R_1 to 116 mm for R_{35}, assuming ice density of 900 kg m^{-3}. Halkola and Puhakka (AGF student report, 2001) reported ice thickness at the DM site on 31 March as 0.86 m, from which the average estimated observed growth rate over 24 days is shown as the dashed line in Figure 4. If all of the tendency for supercooling implicit for the R_5 and R_{35} runs was converted to frazil ice, then incorporated into the ice column, the growth rate curves would coincide with R_1.

[31] A second model diagnostic obtained from the later student observations was the change in mixed layer salinity (Figure 5). The students returned to the DM site, obtaining

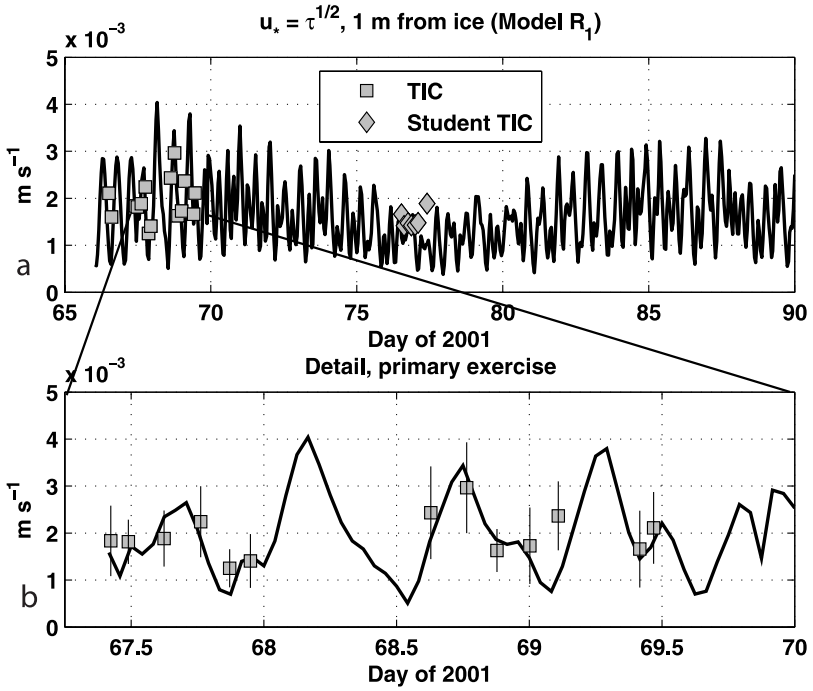

Figure 3. (a) Modeled friction velocity for the entire simulation period, based on moored current meter speed at 10 m depth (solid curve) compared with 3-h average Reynolds stress measurements during the primary March experiment (squares) and later student field exercise (diamonds). (b) Detail during the primary exercise from day 67 to 70. Error bars are ±1 standard deviation of the 15-min turbulence realizations in each 3-h average.

profiles during the period 16–19 March and again on 31 March (Takayama et al., AGF student report, 2001). While the midmonth profiles showed relatively uniform T and S profiles to 40 m (matching closely the R_1 model results) with very slight gradients below, the later profiles showed stronger gradients beginning at 30–35 m depth, probably resulting from advection of saltier water into the site from a source near the mouth of the fjord. In the 1-D model, which had become well mixed to 50 m (the entire vertical domain) by day 80 in all versions, the only source of increased salinity is from ice freezing. The rough correspondence between modeled and observed mixed layer properties thus suggests that this was the main salinity source, commensurate with the ice growth rate calculation. We cannot rule out the possibility that water with differing upper layer properties moved past the DM site during the study; however, the mean vector velocity at 10 m was about 0.01 m s^{-1}, so displacement of the upper layer during the study was small compared with the length of the fjord.

[32] A similar comparison between modeled and observed mixed layer temperatures (Figure 6) better illustrates significant discrepancies between interface submodels with different double-diffusion characteristics. Despite initial mixed-layer temperature 12 mK above freezing, the most active double-diffusive model (R_{35}), reaches a supercooled state near the interface by about midday on 9 March (day 68), during the primary DM exercise when there was no evidence of supercooling or frazil production. For mild double-diffusion (R_5), it takes about 10 days for the mixed layer to reach the surface-pressure freezing point, whereas

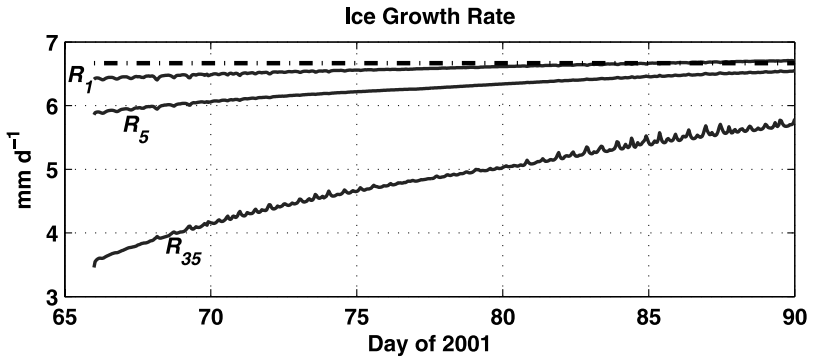

Figure 4. Modeled ice growth rate for three values of R compared with average observed growth rate from 7 to 31 March 2001 (dashed line).

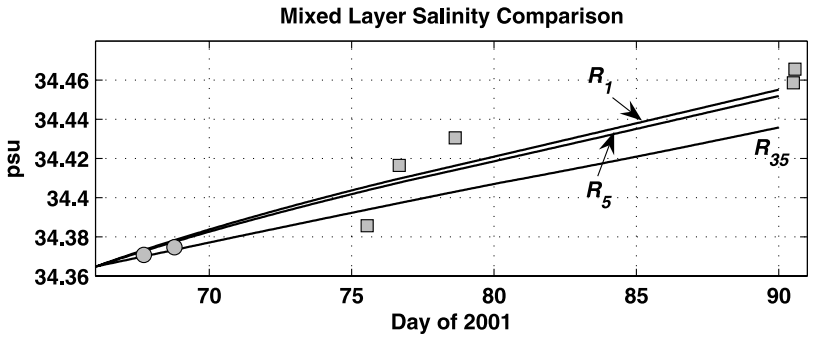

Figure 5. Modeled mixed layer salinity (average, 5–30 m depth) for different values of R compared with daily average TIC data 1 m below ice (circles) and 5–30 m average of salinity profiles at DM site during the later student exercises (squares) from Takayama et al. (AGF student report, 2001).

for no double diffusion (R_1), heat extraction is insufficient to overcome the initial heat content of the upper ocean, and the model remains above freezing throughout the simulation. The midmonth profiles hint at mixed-layer cooling at a slightly slower rate than the R_1 model predicts; however, by the end of the month, the observations show that the upper ocean has warmed to about 16 mK above its surface freezing point. This implies a small source of heat from elsewhere, either from slow advection of warmer water to the site or perhaps from solar radiation penetrating the snow/ice cover.

[33] Modeled versus measured heat flux (Figure 7) provides the most convincing demonstration of the difference between mild double diffusion (R_5) and none (R_1). While there is considerable scatter in the 3-h averages from the 1-m TIC, the R_1 simulation clearly reproduces a good approximation of mean turbulent heat flux during both measurement times. Detail (Figure 7b) reveals that of the three simulations, only R_1 overlaps with the measured heat flux.

[34] Figure 7 illustrates the importance of flux measurements in assessing model performance. If, for example, we had used mixed-layer temperature as the main diagnostic (Figure 6), the presence of a small extraneous heat source (apparently of order one watt per square meter) has an integrated effect on water temperature comparable to the difference between R_1 and R_5. An important point is that even in the presence of other factors that would prevent actual supercooling, if the double-diffusive tendency was as important during freezing as during melting ($R = 35$), the upward heat flux 1 m below the interface would be much larger than we measured. This is implicit in the salinity and heat flux measurements during the primary field program (Figure 2), but there is enough uncertainty in those data to preclude ruling out small values of R. The modeling exercise, on the other hand, indicates that even values as small as $R = 5$ were unlikely.

5. Discussion

[35] The hypothesis driving the late winter Svalbard fjord experiment was that the inherently double-diffusive character of the ice/ocean interface apparent during melting of sea ice is either absent or much weakened when ice freezes. Were this not the case, turbulent heat flux from the ocean would markedly increase under rapidly freezing ice, with a strong potential for supercooling and significant production of frazil crystals, provided adequate nucleation sites were available.

[36] Our observational results from the 2001 VMF campaign, combined with numerical modeling, strongly suggest that R is close to unity (no double diffusion). First, no supercooling or frazil production was observed. Since the well mixed layer beneath the ice was initially above its freezing point, this by itself was not sufficient to rule out mild double diffusion (small R), since as demonstrated by the R_5 model, it might take 10 days or more for the upper ocean to reach a supercooled state (Figure 6). Data from late in March, even after significant additional freezing, suggested a small source of heat from elsewhere that could maintain above freezing temperatures, even in the face of

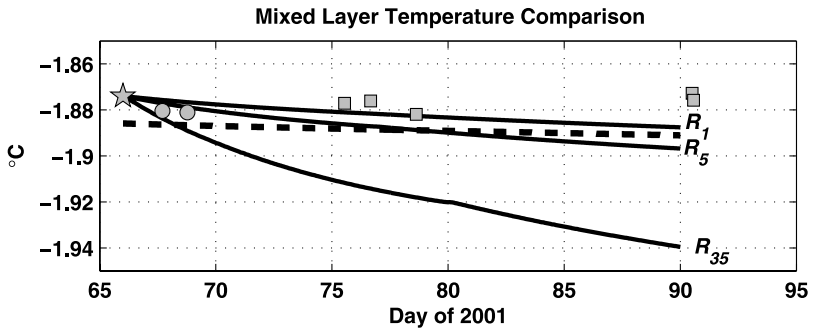

Figure 6. As in Figure 5, except mixed layer temperature. The heavy dashed curve is freezing temperature at surface pressure for the mixed-layer salinity simulation R_1. Freezing temperatures from the other simulations are similar.

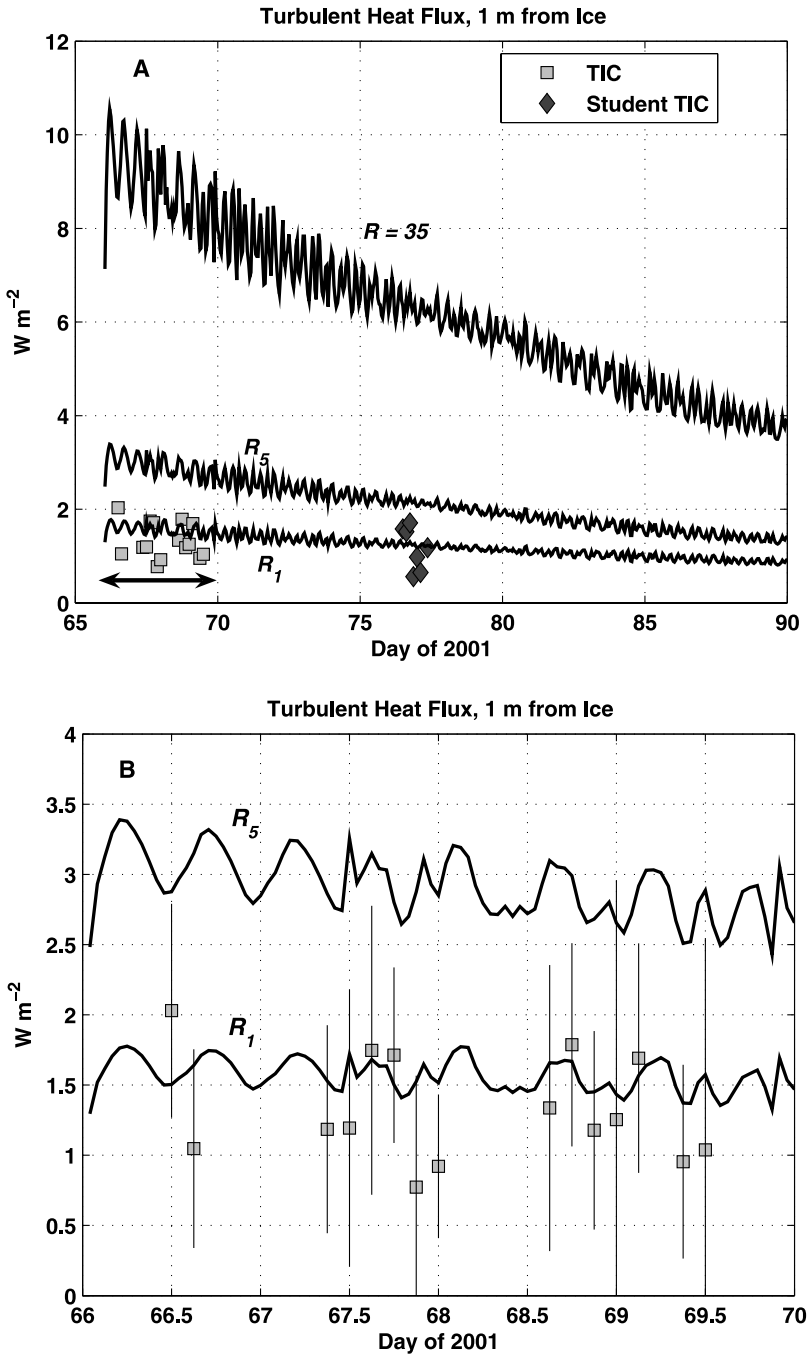

Figure 7. (a) Turbulent heat flux ($\rho c_p \langle w'T' \rangle$) 1 m from the ice for the three model runs (solid curves) for the entire 24-day simulation, plus 3-h averages from the turbulence instrument cluster during the primary campaign (squares) and later student exercise (diamonds). (b) Detail during the primary field experiment in early March (indicated by double arrow in Figure 7a). Error bars represent ±1 standard deviation of the 15-min realizations in each 3-h average.

enhanced heat flux from a mild double-diffusive effect. However, the second factor supporting the hypothesis, namely that measurements of turbulent heat flux 1 m below the ice corresponded closely to the modeled heat flux with $R = 1$, does provide strong evidence that from the point of view of heat flux from the ocean, double diffusion is absent during ice growth. According to the model, even weak double diffusion ($R = 5$) would appreciably increase heat flux to levels well above those measured (Figure 7). We view the absence of supercooling or apparent frazil production during the 2001 VMF exercise, especially when considered in the context of measured heat flux agreeing with model results only when $R = 1$ (Figure 7), as convincing evidence of asymmetry in heat and salt exchange for freezing versus melting.

[37] We stress that the purpose here is to examine melting and freezing at the ice/ocean interface from the perspective of their impact on the dynamics and thermodynamics of the ocean boundary layer. How a solid grows from a liquid solution when the crystal structure cannot accommodate the solute is a fascinating topic but beyond the scope of the present work. It most likely involves relieving double-diffusive tendencies by convection within a mushy layer of ice and saline solution above the advancing ice front [e.g., *Wettlaufer et al.*, 1997; *Feltham et al.*, 2006; *Notz*, 2005].

[38] If the interest is parameterizing heat and salt transfer at an ice/ocean interface in ocean models, results presented here and by *Notz et al.* [2003] have the following ramifications. First, when ice is melting rapidly, as in the marginal ice zone where it can encounter water well above freezing, it is important to recognize the rate limiting function of salt diffusion by including fairly strong double-diffusion strength ($35 \leq R \leq 70$). Depending on the value chosen for R in a particular interface submodel, the numerical value for α_h should be chosen to satisfy the observational constraint of a relatively narrow range of the bulk Stanton number ($0.005 < St_* < 0.006$), along the lines demonstrated in Figure 1.

[39] For freezing, the interface regime is apparently quite different, and the interface submodel should incorporate in some way that the double-diffusive impact on heat extraction from the ocean is much reduced or absent. A recent version of the interface submodel [*McPhee*, 2002, 2008] determines the energy balance at the interface from the last valid time step in the leapfrog scheme, and if ice growth is present, changes R to 1 and sets α_h to St_*. Specifically, the submodel used in section 4 sets $\alpha_h = \alpha_S = 0.0057$ when ice is growing. If instead, the heat balance at the interface dictated melting or no change in ice thickness (conditions never present in the simulations shown here), then $\alpha_h = 0.0093$ and $R = 35$. This particular choice of R (and therefore α_h to satisfy the St_* constraint) at the low end of the range suggested by *Notz et al.* [2003] is somewhat arbitrary. Nevertheless, in our view this approach provides a reasonable description of the present observational state of knowledge, even if lacking aesthetic elegance. As we gain a broader observational base when ice is melting rapidly (also with careful measurement of false bottom migration, including associated fluxes), more precise values for the exchange coefficients should emerge.

[40] **Acknowledgments.** The efforts of UNIS students who continued as part of their course work the measurements begun during the initial field exercise were of great value to this project and are much appreciated. We are grateful for substantial field and logistic support from UNIS. Work was supported by the U.S. National Science Foundation under grants 0324043, 0337813, 0352687 (MGM), and 0082687 (JHM) and by the Research Council of Norway under grants 151447/720, "Atmosphere/Ice/Ocean Interaction Studies." Suggestions for improving the manuscript from two anonymous reviewers are appreciated.

References

Coachman, L. K. (1966), Production of supercooled water during sea ice formation, in *Proceedings of the Symposium on the Arctic Heat Budget and Atmospheric Circulation*, edited by J. O. Fletcher, pp. 497–529, Rand Corp., Santa Monica, Calif.

Feltham, D. L., N. Untersteiner, J. S. Wettlaufer, and M. G. Worster (2006), Sea ice is a mushy layer, *Geophys. Res. Lett.*, *33*, L14501, doi:10.1029/2006GL026290.

Hinze, J. O. (1975), *Turbulence*, 2nd ed., 790 pp., McGraw-Hill, New York.

Holland, M. M., J. A. Curry, and J. L. Schramm (1997), Modeling the thermodynamics of a sea ice thickness distribution: 2. Sea ice/ocean interactions, *J. Geophys. Res.*, *102*, 23,093–23,107, doi:10.1029/97JC01296.

Holland, M. M., C. M. Bitz, and B. Tremblay (2006), Future abrupt reductions in the summer Arctic sea ice, *Geophys. Res. Lett.*, *33*, L23503, doi:10.1029/2006GL028024.

Incropera, F. P., and D. P. DeWitt (1985), *Fundamentals of Heat and Mass Transfer*, 802 pp., John Wiley, New York.

Lewis, E. L., and R. A. Lake (1971), Sea ice and supercooled water, *J. Geophys. Res.*, *76*, 5836–5841, doi:10.1029/JC076i024p05836.

Lewis, E. L., and R. G. Perkin (1983), Supercooling and energy exchange near the Arctic Ocean surface, *J. Geophys. Res.*, *88*, 7681–7685, doi:10.1029/JC088iC12p07681.

Maykut, G. A., and M. G. McPhee (1995), Solar heating of the Arctic mixed layer, *J. Geophys. Res.*, *100*, 24,691–24,703, doi:10.1029/95JC02554.

McPhee, M. G. (1992), Turbulent heat flux in the upper ocean under sea ice, *J. Geophys. Res.*, *97*, 5365–5379, doi:10.1029/92JC00239.

McPhee, M. G. (1999), Scales of turbulence and parameterization of mixing in the ocean boundary layer, *J. Mar. Syst.*, *21*, 55–65, doi:10.1016/S0924-7963(99)00005-6.

McPhee, M. G. (2002), Turbulent stress at the ice/ocean interface and bottom surface hydraulic roughness during the SHEBA drift, *J. Geophys. Res.*, *107*(C10), 8037, doi:10.1029/2000JC000633.

McPhee, M. G. (2008), Physics of early summer ice/ocean exchanges in the western Weddell Sea during ISPOL, *Deep Sea Res. II*, *55*(819), 1075–1089, doi:10.1016/j.dsr2.2007.12.022.

McPhee, M. G., G. A. Maykut, and J. H. Morison (1987), Dynamics and thermodynamics of the ice/upper ocean system in the marginal ice zone of the Greenland Sea, *J. Geophys. Res.*, *92*, 7017–7031, doi:10.1029/JC092iC07p07017.

McPhee, M. G., T. P. Stanton, J. Morison, and D. Martinson (1998), Freshening of the upper ocean in the Arctic: Is perennial sea ice disappearing?, *Geophys. Res. Lett.*, *25*, 1729–1732, doi:10.1029/98GL00933.

McPhee, M. G., C. Kottmeier, and J. H. Morison (1999), Ocean heat flux in the central Weddell Sea in winter, *J. Phys. Oceanogr.*, *29*, 1166–1179, doi:10.1175/1520-0485(1999)029<1166:OHFITC>2.0.CO;2.

McPhee, M. G., T. Kikuchi, J. H. Morison, and T. P. Stanton (2003), Ocean-to-ice heat flux at the North Pole environmental observatory, *Geophys. Res. Lett.*, *30*(24), 2274, doi:10.1029/2003GL018580.

Mellor, G. L., M. G. McPhee, and M. Steele (1986), Ice-seawater turbulent boundary layer interaction with melting or freezing, *J. Phys. Oceanogr.*, *16*, 1829–1846, doi:10.1175/1520-0485(1986)016<1829:ISTBLI>2.0.CO;2.

Morison, J. H., and M. McPhee (2001), Ice-ocean interaction, in *Encyclopedia of Ocean Sciences*, edited by J. Steele, S. Thorpe, and K. Turekian, pp. 1271–1281, Elsevier, New York.

Notz, D. (2005), Thermodynamic and fluid-dynamical processes in sea ice, Ph.D. dissertation, Trinity Coll., Cambridge Univ., Cambridge, UK.

Notz, D., M. G. McPhee, M. G. Worster, G. A. Maykut, K. H. Schlünzen, and H. Eicken (2003), Impact of underwater-ice evolution on Arctic summer sea ice, *J. Geophys. Res.*, *108*(C7), 3223, doi:10.1029/2001JC001173.

Owen, P. R., and W. R. Thomson (1963), Heat transfer across rough surfaces, *J. Fluid Mech.*, *15*, 321–334, doi:10.1017/S0022112063000288.

Perovich, D. K., and B. Elder (2002), Estimates of ocean heat flux at SHEBA, *Geophys. Res. Lett.*, *29*(9), 1344, doi:10.1029/2001GL014171.

Rothrock, D. A., Y. Yu, and G. A. Maykut (1999), Thinning of the Arctic ice cover, *Geophys. Res. Lett.*, *26*, 3469–3472, doi:10.1029/1999GL010863.

Steele, M., G. L. Mellor, and M. G. McPhee (1989), Role of the molecular sublayer in the melting or freezing of sea ice, *J. Phys. Oceanogr.*, *19*, 139–147, doi:10.1175/1520-0485(1989)019<0139:ROTMSI>2.0.CO;2.

Untersteiner, N., and R. Sommerfeld (1964), Supercooled water and bottom topography of floating ice, *J. Geophys. Res.*, *69*, 1057–1062, doi:10.1029/JZ069i006p01057.

Weeks, W. F., and S. F. Ackley (1986), The growth, structure, and properties of sea ice, in *The Geophysics of Sea Ice*, edited by N. Untersteiner, pp. 9–164, Plenum, New York.

Wettlaufer, J. S., M. G. Worster, and H. E. Huppert (1997), Natural convection during solidification of an alloy from above with application to the evolution of sea ice, *J. Fluid Mech.*, *344*, 291–316, doi:10.1017/S0022112097006022.

Yaglom, A. M., and B. A. Kader (1974), Heat and mass transfer between a rough wall and turbulent flow at high Reynolds and Peclet numbers, *J. Fluid Mech.*, *62*, 601–623, doi:10.1017/S0022112074000838.

M. G. McPhee, McPhee Research Company, 450 Clover Springs Road, Naches, WA 98937, USA. (mmcphee@starband.net)

J. H. Morison, Polar Science Center, University of Washington, 1013 NE 40th Street, Seattle, WA 98105, USA.

F. Nilsen, University Centre in Svalbard, P. O. Box 156, N-9171 Longyearbyen, Norway.